

# Characterization of Electrical Behavior of Ba<sub>5</sub>HoTi<sub>3</sub>V<sub>7</sub>O<sub>30</sub> Ceramic Using Impedance Analysis

Kiran Kathayat<sup>1\*</sup>, Anuradha Panigrahi<sup>2</sup>, Arvind Pandey<sup>3</sup>, Susmita Kar<sup>1</sup>

<sup>1</sup>Department of Physics, North Orissa University, Baripada, India; <sup>2</sup>Department of Physics, D.N. College, Itanagar, India; <sup>3</sup>Department of Physics, North Eastern Regional Institute of Science & Technology, Nirjuli, India.  
Email: \*kathayatkiran@yahoo.in, kathayatkiran@gmail.com

Received March 12<sup>th</sup>, 2012; revised April 16<sup>th</sup>, 2012; accepted May 19<sup>th</sup>, 2012

## ABSTRACT

Polycrystalline sample of Ba<sub>5</sub>HoTi<sub>3</sub>V<sub>7</sub>O<sub>30</sub> was prepared using solid-state reaction technique. X-ray structural analysis indicated a single-phase formation with orthorhombic structure. Microstructural study by SEM showed non-uniform distribution of grains over the surface of the sample. Impedance and modulus spectroscopy studies were carried out, as functions of frequency (42 Hz - 5 MHz) and temperature (RT-773K). The Nyquist plots clearly showed the presence of both bulk and grain boundary effect in the compound. Electrical phenomena in the material can appropriately be modeled in terms of an equivalent circuit with R, C and CPE in parallel. The fitting procedure used here allows us to determine the value of R and C with good precision. Here R<sub>2</sub> and R<sub>3</sub> correspond to the resistance contributed from the grain boundary and bulk, respectively. C<sub>1</sub> and C<sub>2</sub> correspond to the capacitance contributed from the grain boundary and bulk, respectively. The real part of electrical modulus shows that the material is highly capacitive. The asymmetric peak of the imaginary part of electric modulus M'', predicts a non Debye type relaxation. The activation energy of the compound (calculated both from impedance and modulus spectrum) is same, and hence the relaxation process may be attributed to the same type of charge carriers.

**Keywords:** Ceramics; X-Ray Diffraction; Impedance Spectroscopy; Electrical Properties

## 1. Introduction

Ferroelectric compounds of tungsten bronze (TB) structural family covers a large number of ferroelectric materials which are found to be useful for applications in various electronic devices such as transducers, actuators, capacitors, and ferroelectric random access memory [1,2]. They have also some associated properties like pyroelectric, piezoelectric, and nonlinear optical properties [3-5]. The TB structure consists of a skeleton framework of distorted BO<sub>6</sub> octahedral sharing corners in such a way that a variety of cations can be substituted at three different types of interstices (A, B, and C) of a general formula (A<sub>1</sub>)<sub>2</sub>(A<sub>2</sub>)<sub>4</sub>(C<sub>4</sub>)(B<sub>1</sub>)<sub>2</sub>(B<sub>2</sub>)<sub>8</sub>O<sub>30</sub>. Thus it provides scope for improving the ferroelectric properties in search of new and better materials for device applications .where A-type (mono or divalent) cations can be accommodated at different types of interstitial (A<sub>1</sub>, A<sub>2</sub>) sites. Tri- or pentavalent atoms are substituted at octahedral sites B<sub>1</sub> and B<sub>2</sub> [2]. The C site (smallest interstice) is generally empty.

Detailed literature study reveals that a lot of work has been carried out on ferroelectric niobates, vanadates and

tantalates having TB structure [6-9] such as, Ba<sub>5</sub>RTi<sub>3-x</sub>Zr<sub>x</sub>Nb<sub>7</sub>O<sub>30</sub> (x = 0, 1, 2, 3) [10,11], Ba<sub>5</sub>RTi<sub>3</sub>Nb<sub>10</sub>O<sub>30</sub> (R = Dy and Sm) [12], Ba<sub>5-x</sub>Sr<sub>x</sub>DyTi<sub>3</sub>V<sub>7</sub>O<sub>30</sub> (x = 0 - 5) [13], Sr<sub>5</sub>EuCr<sub>3</sub>Nb<sub>7</sub>O<sub>30</sub> [14], Ba<sub>4</sub>SrRTi<sub>3</sub>V<sub>7</sub>O<sub>30</sub> (R = Sm, Dy) [15]. These compounds show many interesting properties like diffuse phase transition with wide variation of transition temperature. One such compound which has drawn our attention is Ba<sub>5</sub>HoTi<sub>3</sub>V<sub>7</sub>O<sub>30</sub> (BHTV) which has already been examined elsewhere [16] and some of its properties have been reported. To know more about this compound and to explore its application, we have summarized the structural, impedance and modulus properties of the BHTV compound in this paper.

## 2. Experimental

Preparation of the material. A polycrystalline sample of BHTV was fabricated using solid state reaction technique. Powders of BaCO<sub>3</sub> (Loba chemie, 99%), Ho<sub>2</sub>O<sub>3</sub> (Merck, 99.5%+), TiO<sub>2</sub> (Loba chemie, 99.5%) and V<sub>2</sub>O<sub>5</sub> (Loba chemie, 99%) in stoichiometric proportion were weighed and thoroughly ground in an agate mortar to maintain proper stoichiometry and homogeneity in mixture, and then calcined at 1023 K for 12 hrs. The calcined powder

\*Corresponding author.

was pressed into cylindrical pellets 12 - 13 mm in diameter and 1 - 2 mm thick under the pressure of 7 tons using a hydraulic press. Polyvinyl butyral (PVB) was used as a binder to reduce the brittleness of the pellets, which was burnt out during sintering. The pellets were then sintered in an air atmosphere at 1073 K for 12 hrs, and then polished with fine emery paper to make their faces flat and parallel. The pellets were finally coated with conductive silver paint and dried at 423 K for 2 hour before carrying out impedance measurements.

Characterization of the material. X-ray diffraction (XRD) studies of the materials were carried out at room temperature in the Bragg angle range 20° - 80° by Rigaku X-ray diffractometer (model: Miniflex). Surface morphology of the compound was studied by scanning electron microscopy (JEOL JSM-5800F). The impedance measurements were carried out at an input signal level of 300 mV in the temperature range of RT-773 K using a computer-controlled impedance analyzer (HIOKI LCR Hi TESTER, Model: 3532-50) in the frequency range of 42 Hz - 5 MHz along with a laboratory made sample holder and a heating arrangement.

### 3. Results and Discussion

#### 3.1. Structural Study

The room temperature XRD patterns (**Figure 1**) of the

calcined powder of BHTV show the formation of single-phase compound with orthorhombic crystal structure. The reflection peaks of the patterns were indexed in tetragonal or orthorhombic crystal system using computer software "POWDMULT" [17] (Since TB compounds have generally tetragonal or orthorhombic crystal structure). The position of the strongest peak in this compound is around 30°. An orthorhombic unit cell was selected on the basis of the best agreement between observed and calculated interplanar spacing  $d$  (*i.e.*,  $\sum \Delta d = \sum (d_{\text{obs}} - d_{\text{cal}}) = \text{minimum}$ ) for this compound. The unit cell parameters of this compound are  $a = 13.5479 \text{ \AA}$ ,  $b = 8.3346 \text{ \AA}$  and  $c = 5.6697 \text{ \AA}$ . The crystallite size ( $D_{hkl}$ ) of the powder sample was estimated from the broadening of the peaks ( $\beta_{1/2}$ ), using Debye-Scherrer's equation [18];  $D_{hkl} = 0.89\lambda / (\beta_{1/2} \cos \theta_{hkl})$ , where  $\lambda = 1.5405 \text{ \AA}$  and  $\theta_{hkl}$  = Bragg angle. Broadening due to mechanical strain, instrumental error and other factors was ignored during calculation. The average crystallite size of BHTV was found to be 16.61 nm.

The inset of **Figure 1** shows the scanning electron micrograph of the BHTV pellet at room temperature. It is found that the grains are of platelet like morphology and size are non-uniform and densely distributed throughout the sample. A certain degree of porosity persists which may be due to the low sintering temperature. The average grain size of the compound was found as  $\sim 3 \mu\text{m}$ . The

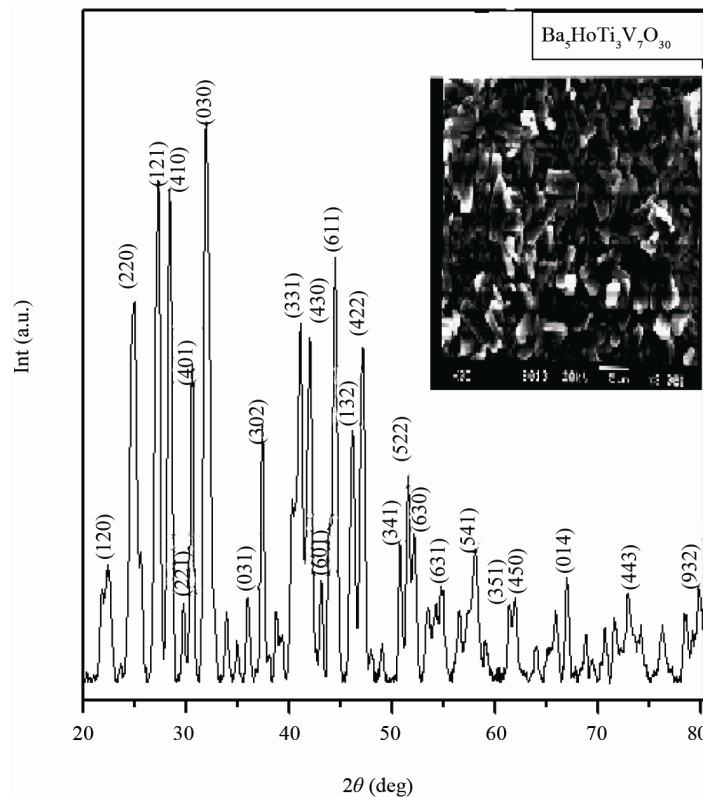


**Figure 1. Room temperature XRD pattern and SEM micrograph (inset) of BHTV.**

shape, size and distribution of grains in the microstructure suggest that the sample has polycrystalline nature. Similar microstructures are observed with that of some other materials of this family [13].

### 3.2. Electrical Analysis

Complex impedance analysis technique is an important and powerful tool to investigate the electrical properties of materials over a wide range of frequency (42 Hz - 5 MHz) and temperature (573 K - 773 K). **Figure 2** shows the Nyquist plots (symbol ■) through experiment and

fitted data (symbol □) for 573 K, 623 K, 673 K and 723 K temperature by Equation (1) below:

$$Z(\omega) = R_1 + \left( \frac{R_2}{1 + Z_{CPE1}^{-1} R_2 + j\omega C_1 R_2} \right) + \left( \frac{R_3}{1 + Z_{CPE2}^{-1} R_3 + j\omega C_2 R_3} \right) \tag{1}$$

where  $Z_{CPE} = 1 / [(j\omega)^\alpha C]$  and Bode plot ( $Z$  experimental ■ and calculated □ vs log frequency) is shown in

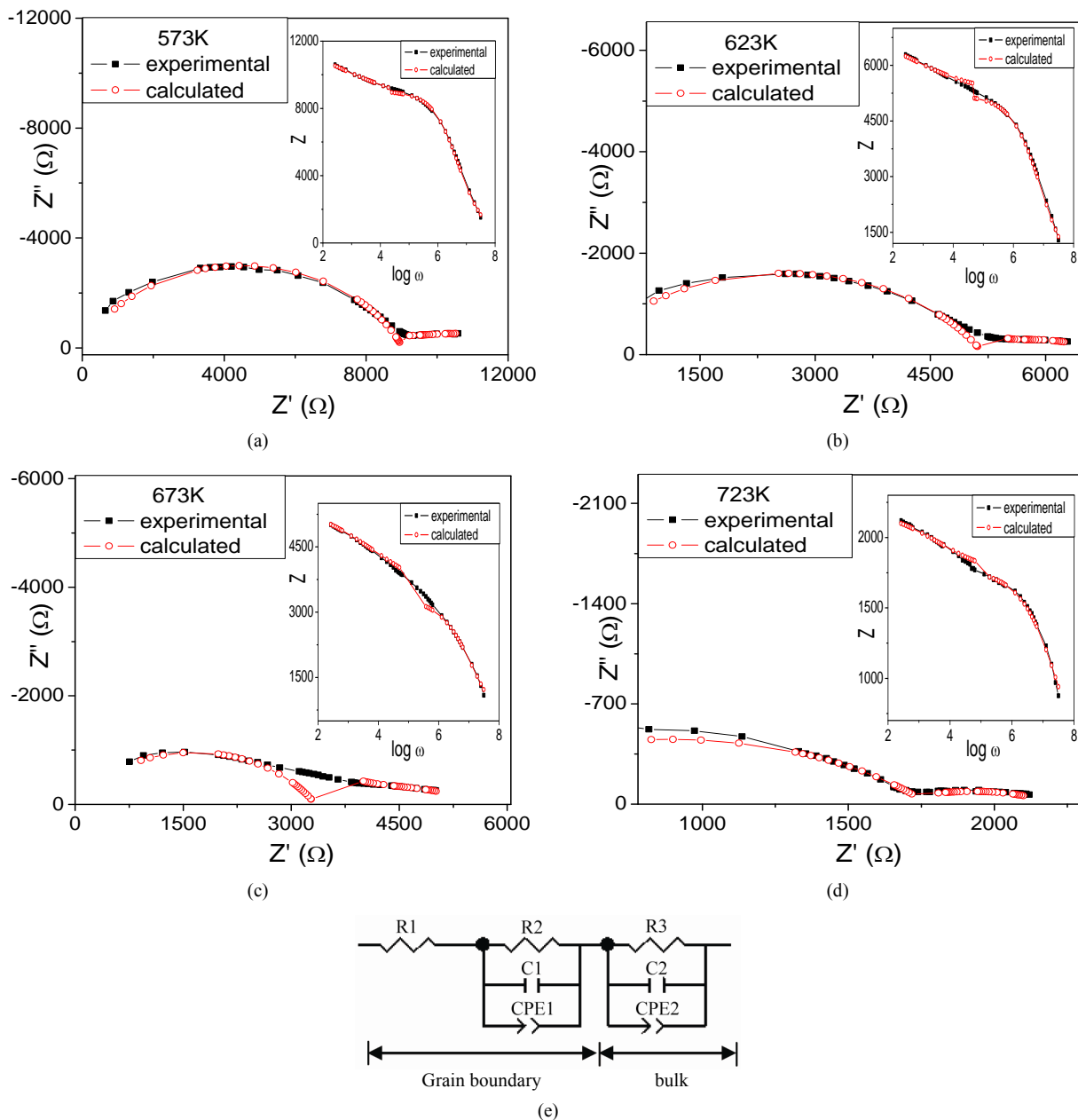


**Figure 2.** Nyquist plots (symbol ■) through experiment and fitted data (symbol □) for (a) 573 K; (b) 623 K; (c) 673 K and (d) 723 K temperature; (e) model to an equivalent circuit used in fitting.

inset of **Figures 2(a)-(d)**. The complex impedance plots (**Figure 2**) for all mentioned temperature comprise of two semicircular arcs (due to bulk at high frequency and grain boundary at low frequency) with center below the real axis suggesting the departure from ideal Debye behavior. This departure is due to the presence of constant phase element (CPE) in RC system. CPE is used in a model to compensate non-homogeneity in the system. For a rough or porous surface,  $\alpha$  value is between 0.9 and 1 which can cause a double-layer capacitance to appear as a constant phase element. If  $\alpha$  equals to 1 than the equation is identical to that of a capacitor and if  $\alpha$  is 0 then  $Z$  is equals to  $R/2$  resemble to ideal resistor. The CPE can also yield to an inductance, if  $\alpha = -1$ . For ideal Debye-like response, the equivalent circuit comprises of a parallel combination of a resistor and capacitor with single relaxation time. Here, in **Figure 2(e)** a single semicircular arc can be modeled to an equivalent circuit of parallel combination of a resistance, capacitance along with a constant phase element [19]. The values of the temperature dependent electrical parameters corresponding to the equivalent circuit (shown in **Figure 2(e)**) are given in **Table 1**.

**Figure 3(a)** shows the variation of imaginary part of impedance ( $Z''$ ) with frequency at different temperatures. The  $Z''$ -frequency patterns exhibits some important features such as; 1) the value of  $Z''_{\max}$  (*i.e.*, peak value) shifts towards higher frequency on increasing temperature; 2) appearance of a peak at a particular frequency (known as relaxation frequency,  $f_{\max}$ ); 3) the peak value of  $Z''$  decreases as the temperature increases and 4) the peaks in the plot could be observed upto a temperature of 673K. Beyond this temperature peaks could not be observed because it shifts towards higher frequencies which overshoots the limits in which our measurements have been carried out. These features may be considered due to occurrence of the temperature-dependent relaxation phenomena in the materials [20].

**Figure 3(b)** shows the variation of the real part of the impedance  $Z'$  as a function of the frequency at various temperatures (573 K - 773 K) for BHTV. It is observed that  $Z'$  decreases as temperature increases, indicating a negative temperature coefficient of the resistance in the system. The plateau region of the plot also indicates the

presence of a relaxation process in the material.

**Figure 4** shows the variation of relaxation times as a function of inverse of absolute temperature of BHTV compound. In a relaxation system, the relaxation times ( $\tau$ ) were calculated from impedance ( $Z''$ ) and modulus ( $M''$ )

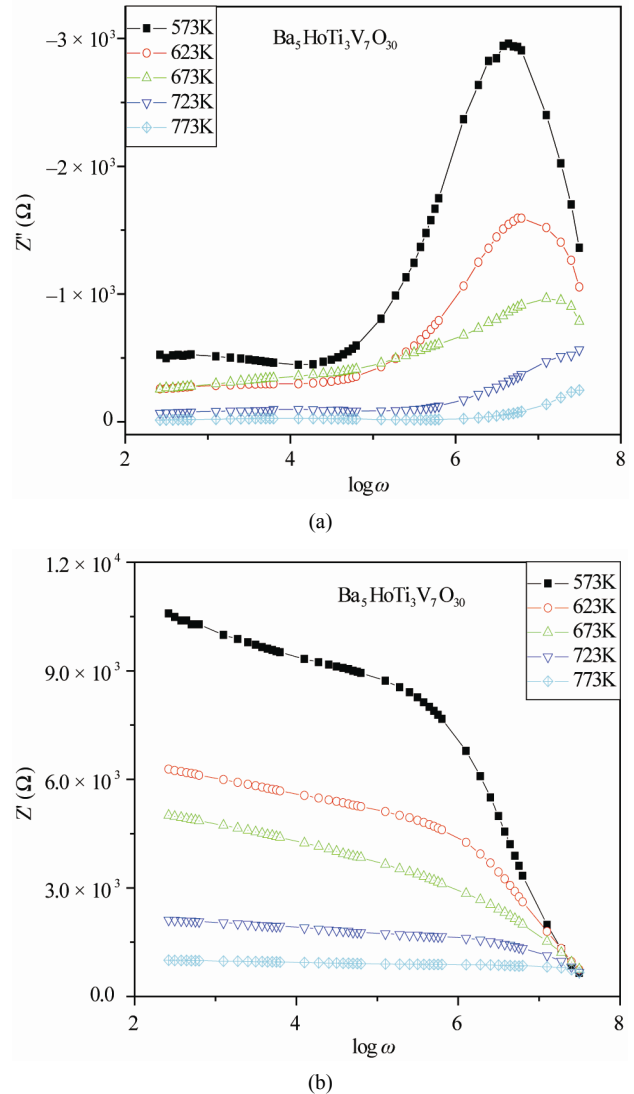


**Figure 3. (a) Variation of imaginary part of impedance ( $Z''$ ) and (b) real part of the impedance  $Z'$  with frequency at different temperatures.**

**Table 1. The values of the temperature dependent electrical parameters corresponding to the equivalent circuit.**

Temp (K)	Electrical parameters									
	$R_1$	$R_2$	CPE1	$\alpha_1$	$C_1$	$R_3$	CPE2	$\alpha_2$	$C_2$	
573 K	7733	5999	$5.6093e^{-5}$	0.22	$1.099e^{-9}$	9037	$1.6e^{-9}$	0.74	$0.258e^{-12}$	
623 K	5277	1540	$4.3987e^{-5}$	0.4	$56.985e^{-9}$	5200	$3.5e^{-9}$	0.7	$0.184e^{-12}$	
673 K	2911	2810	$2.6472e^{-5}$	0.28	$1.957e^{-9}$	3340	$8.5e^{-9}$	0.65	$0.640e^{-12}$	
723 K	1722	485	$6.7185e^{-5}$	0.41	$22.685e^{-9}$	1773	$2e^{-8}$	0.6	$0.040e^{-12}$	

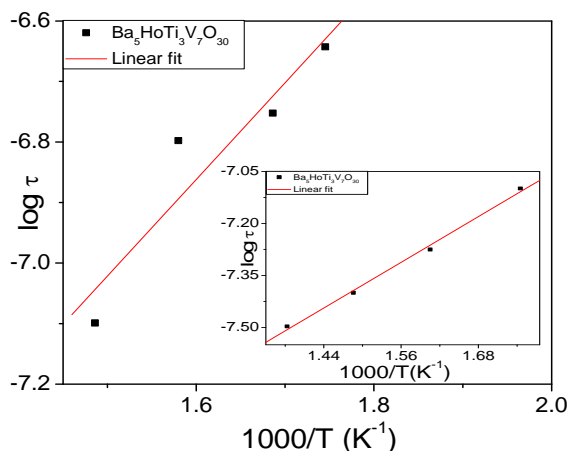


**Figure 4.** Variation of relaxation times as a function of inverse of absolute temperature calculated from the impedance spectrum ( $Z''$  vs. frequency) and modulus spectrum ( $M''$  vs. frequency) (inset).

data by using the relation:  $\tau = 1/\omega = 1/2\pi f_{\max}$ ; where  $f_{\max}$  is the relaxation frequency. It was observed that the value of  $\tau$  was found to be decreasing with increase in temperature, which is a typical semiconductor behavior of the sample. The activation energy ( $E_a$ ) of the compound was calculated from the Arrhenius equation [21, 22];  $\tau = \tau_0 \exp(-E_a/K_B T)$ , Where,  $\tau_0$  is the pre exponential factor,  $K_B$  is Boltzmann constant and  $T$  is the absolute temperature. The value of the activation energy, obtained from the slope of the curve in the plot of  $\log \tau$  against  $10^3 T^{-1}$ , is found to be  $\sim 0.34$  eV (From impedance plot) and  $\sim 0.22$  eV (From modulus plot, inset). It is clear that the activation energy of the compound (as calculated from the impedance and modulus spectra) is nearly the same, and the relaxation process may be attributed to the same type of charge carriers.

### 3.3. Modulus Analysis

An electrical response of the samples can be analyzed via complex dielectric modulus formalism  $M''$  which is another approach based on polarization analysis. Complex impedance spectrum gives emphasis to elements with the larger resistance whereas complex modulus plots highlight those with smaller capacitance. **Figures 5(a) and (b)** ( $M'$  vs  $M''$ ) depicts that the modulus plane shows a single semicircle for BHTV at higher temperatures ( $\geq 473$  K). Although, at first sight, there appears a single semicircular arc in modulus spectra at lower temperatures ( $\leq 473$  K) of these compounds as well, however, further resolution of these spectra at low frequencies reveal two semicircular arcs. The small semicircle in the  $M$  vs  $M''$  plot corresponds to the high capacitance values. The arc at low frequency is due to the grain boundary whereas the higher frequency arc depicts the bulk effect. With rise in tem-

peratures, both grain and grain boundary effect appears to merge into the single semicircle. The modulus spectrum shows a marked change in its shape with rise in temperature suggesting a change in the capacitance values of the material. The semicircle in higher frequency region is not complete due to the frequency limit of the measuring instrument (maximum 5 MHz). The intercept on the real axis indicates the total capacitance contributed by the grain and grain boundary.

**Figure 5(c)** shows the variation of  $M'$  as a function of frequency for BHTV in a wide temperatures range (373 K - 773 K). This shows that  $M'$  approaches to zero in the low frequency region, and a continuous dispersion on increasing frequency may be contributed to the conduction phenomena due to short range mobility of charge carriers. This implies the lack of a restoring force for flow of charge under the influence of a steady electric field [20]. This confirms elimination of electrode effect in the material.

**Figure 5(d)** shows the variation of imaginary part of electric modulus with frequency for BHTV at different temperatures 373 K - 773 K. The electrical modulus maxima ( $M''_{\max}$ ) shifts towards higher frequencies side with rise in temperature ascribing correlation between motions of mobile ions [23]. The asymmetric peak broadening shows that the relaxation is of non-Debye type which can be concluded due to the spreading of relaxation times with different time constant. The low frequency peaks shows that the ions can move over long distances whereas high frequency peaks merge to spatially confinement of ions in their potential well. The nature of modulus spectrum suggests the existence of hopping mechanism of electrical conduction in the material.

The scaling behavior of normalized imaginary  $M$  has been shown in **Figure 5(e)** at selected temperatures. The coincidence of all the curves of different temperatures into a single master curve indicates temperature independence of dynamic processes [24,25]. The scaling behavior of the electric modulus of the compounds shows that there is not perfect overlapping of different temperature data peaks. This depicts that different relaxation processes are occurring in the compounds. It is to be noted that all the plots have a similar shape with a long and flat tail extending from the low-frequency region up to the intermediate frequency region. The presence of a flat tail is associated with the grain boundary effect while that part of the peaking curve observed at higher frequencies is due to the bulk effect. There is both electronic and ionic contribution in BHTV compound. BHTV is less dispersed (**Figure 5(e)**) which indicates that conductivity in this compound is dominated by one type of species. Since, BHTV have shown strong ionic character (as revealed by impedance plots) [16], thus, it can be presumed that here in case of this compound ionic contribution is

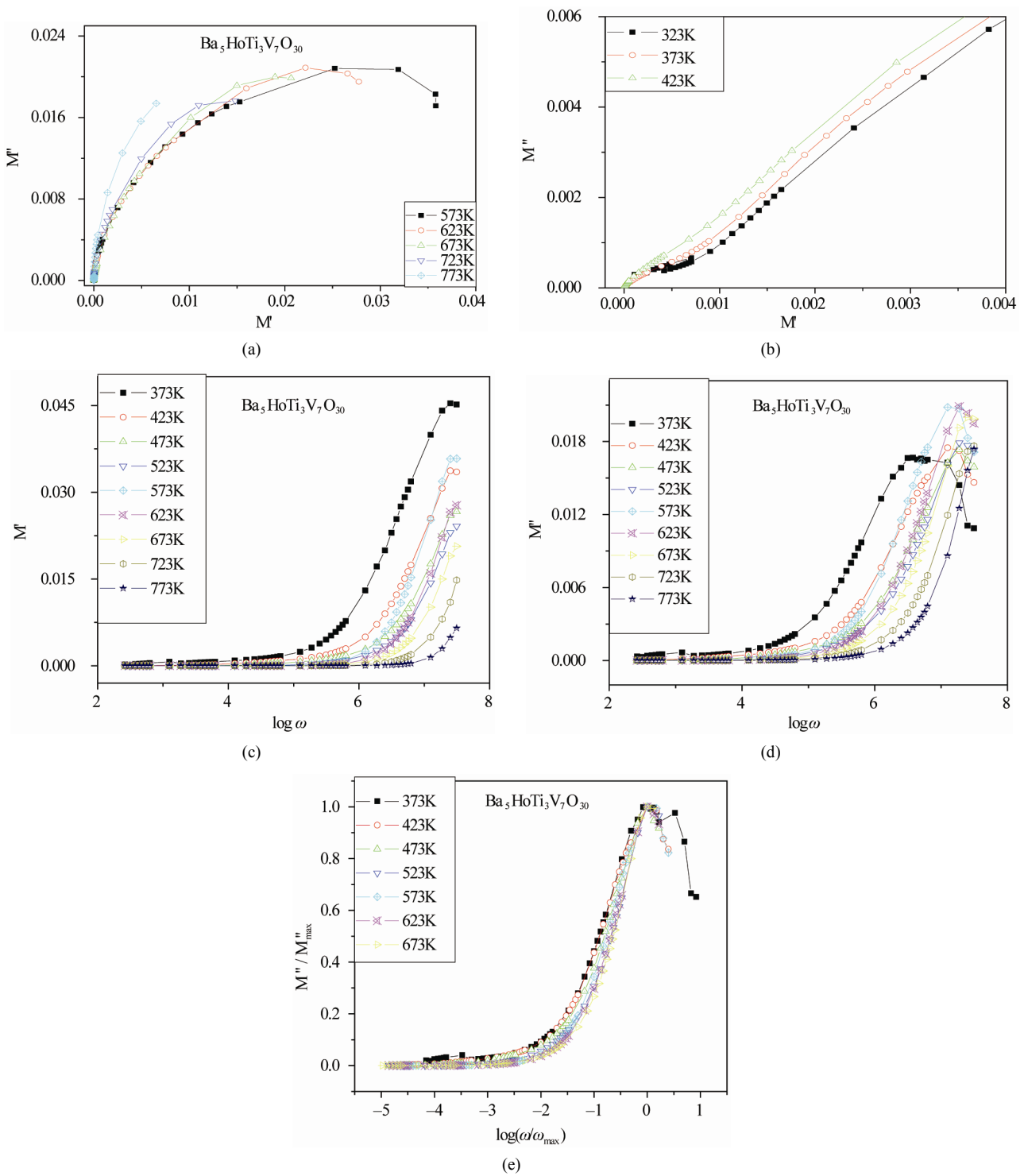


Figure 5. (a), (b)  $M'$  Vs  $M''$ ; (c)  $\log \omega$  vs  $M'$ ; (d)  $\log \omega$  vs  $M''$ ; (e)  $\log(\omega/\omega_{max})$  vs  $M''/M''_{max}$  of BHTV at different temperatures.

dominating over the electronic contribution.

#### 4. Conclusion

The polycrystalline sample of BHTV is prepared by solid state reaction. Preliminary X-ray analysis confirms the

orthorhombic crystal structure at room temperature. The surface morphology of the compound is studied through SEM, which gives the average grain size as the order of 3  $\mu\text{m}$ . From the impedance and modulus spectroscopic studies the material showed relaxation effects which are of non-Debye type. The relaxation frequencies shifted to

higher frequency side with increase in temperature. The complex impedance plots reveal the contribution of bulk and grain boundary in it. The activation energy is found to be 0.34 eV (from impedance plot) and 0.22 eV (from modulus plot) are nearly same, and hence the relaxation process may be attributed to the same type of charge carriers. Modulus spectra indicate that there is both electronic and ionic contribution in BHTV compound.

## 5. Acknowledgements

Authors thank Director, NERIST to permit to carry out research work and for his encouragement and help. We are grateful to the CRF of IIT, Kharagpur and Dr S. R. Shanigrahi (IMRE, Singapore) for their help in carrying out SEM and XRD, respectively.

## REFERENCES

- [1] R. R. Neurgaonkar, J. G. Nelson and J. R. Oliver, "Ferroelectric Properties of the Tungsten Bronze  $M^{2+}M^{4+}_2Nb_8O_{30}$  Solid Solution Systems," *Materials Research Bulletin*, Vol. 27, No. 6, 1992, pp. 677-684. [doi:10.1016/0025-5408\(92\)90074-A](https://doi.org/10.1016/0025-5408(92)90074-A)
- [2] R. R. Neurgaonkar and W. K. Cory, "Progress in Photorefractive Tungsten Bronze Crystals," *Journal of Optical Society of America B*, Vol. 3, No. 2, 1986, pp. 274-282. [doi:10.1364/JOSAB.3.000274](https://doi.org/10.1364/JOSAB.3.000274)
- [3] C. Huang, A. S. Bhalla and R. Guo, "Measurement of Microwave Electro-Optic Coefficient in Sr<sub>0.61</sub>Ba<sub>0.39</sub>Nb<sub>2</sub>O<sub>6</sub> Crystal Fiber," *Applied Physics Letters*, Vol. 86, No. 21, 2005, Article ID: 211907. [doi:10.1063/1.1937997](https://doi.org/10.1063/1.1937997)
- [4] Y. Yuan, X. M. Chen and Y. J. Wu, "Diffused Ferroelectrics of Ba<sub>6</sub>Ti<sub>2</sub>Nb<sub>8</sub>O<sub>30</sub> and Sr<sub>6</sub>Ti<sub>2</sub>Nb<sub>8</sub>O<sub>30</sub> with Filled Tungsten-Bronze Structure," *Journal of Applied Physics*, Vol. 98, No. 8, 2005, Article ID: 084110. [doi:10.1063/1.2120891](https://doi.org/10.1063/1.2120891)
- [5] M. R. Ranga Raju, R. N. P. Choudhary and H. R. Rukmini, "Diffuse Phase Transition in Sr<sub>3</sub>RTi<sub>3</sub>Nb<sub>7</sub>O<sub>30</sub> (R = La, Nd, Sm, Gd and Dy) Ferroelectric Ceramics," *Ferroelectrics*, Vol. 325, No. 1, 2005, pp. 25-32. [doi:10.1080/00150190500326720](https://doi.org/10.1080/00150190500326720)
- [6] P. S. Sahoo, A. Panigrahi, S. K. Patri and R. N. P. Choudhary, "Structural and Electrical Properties of Ba<sub>5</sub>SmTi<sub>3</sub>-V<sub>7</sub>O<sub>30</sub> Ceramics," *Journal of Material Science: Material in Electronics*, Vol. 21, No. 2, 2010, pp. 160-167. [doi:10.1007/s10854-009-9887-2](https://doi.org/10.1007/s10854-009-9887-2)
- [7] M. R. R. Raju and R. N. P. Choudhary, "Structural, Dielectric and Electrical Properties of Sr<sub>3</sub>RTi<sub>3</sub>Nb<sub>7</sub>O<sub>30</sub> (R = Gd and Dy) Ceramics," *Materials Letters*, Vol. 57, No. 19, 2003, pp. 2980-2987. [doi:10.1016/S0167-577X\(02\)01408-8](https://doi.org/10.1016/S0167-577X(02)01408-8)
- [8] P. Ganguly, A. K. Jha and K. L. Deori, "Investigations of Dielectric, Pyroelectric and Electrical Properties of Ba<sub>5</sub>-SmTi<sub>3</sub>Nb<sub>7</sub>O<sub>30</sub> Ferroelectric Ceramic," *Journal of Alloys and Compounds Volume*, Vol. 484, No. 1-2, 2009, pp. 40-44. [doi:10.1016/j.jallcom.2009.05.034](https://doi.org/10.1016/j.jallcom.2009.05.034)
- [9] V. Hornebecq, C. Elissalde, J. M. Reau and J. Ravez, "Relaxations in New Ferroelectric Tantalates with Tetragonal Tungsten Bronze Structure," *Ferroelectrics*, Vol. 238, No. 1, 2000, pp. 57-63. [doi:10.1080/00150190008008767](https://doi.org/10.1080/00150190008008767)
- [10] N. K. Singh, R. N. P. Choudhary and A. Panigrahi, "Phase Transition of Ba<sub>5</sub>SmTi<sub>3-x</sub>Zr<sub>x</sub>Nb<sub>7</sub>O<sub>30</sub> (x = 0, 1, 2, 3) Ferroelectric Ceramics," *Journal of Materials Science Letters*, Vol. 20, No. 8, 2001, pp. 707-712. [doi:10.1023/A:1010906907512](https://doi.org/10.1023/A:1010906907512)
- [11] N. K. Singh, A. Panigrahi and R. N. P. Choudhary, "Structural and Dielectric Properties of Ba<sub>5</sub>EuTi<sub>3-x</sub>Zr<sub>x</sub>Nb<sub>7</sub>O<sub>30</sub> Relaxor Ferroelectrics," *Materials Letters*, Vol. 50, No. 1, 2001, pp. 1-5. [doi:10.1016/S0167-577X\(00\)00402-X](https://doi.org/10.1016/S0167-577X(00)00402-X)
- [12] S. R. Shannigrahi, R. N. P. Choudhary, A. Kumar and H. N. Acharya, "Phase Transition in Ba<sub>5</sub>RTi<sub>3</sub>Nb<sub>7</sub>O<sub>30</sub> (R = Dy, Sm) Ferroelectric Ceramics," *Journal of Physics and Chemistry of Solids*, Vol. 59, No. 5, 1998, pp. 737-742. [doi:10.1016/S0022-3697\(97\)00217-5](https://doi.org/10.1016/S0022-3697(97)00217-5)
- [13] P. S. Sahoo, A. Panigrahi, S. K. Patri and R. N. P. Choudhary, "Effect of Strontium Substitution on Electrical Conduction Properties of Ba<sub>5</sub>DyTi<sub>3</sub>V<sub>7</sub>O<sub>30</sub>," *The European Physical Journal Applied Physics*, Vol. 52, No. 3, 2010, Article ID: 30601. [doi:10.1051/epjap/2010146](https://doi.org/10.1051/epjap/2010146)
- [14] M. R. R. Raju, R. N. P. Choudhary and S. Ram, "Dielectric and Electrical Properties of Sr<sub>5</sub>EuCr<sub>3</sub>Nb<sub>7</sub>O<sub>30</sub> Nanoceramics Prepared Using a Novel Chemical Route," *Physica Status Solidi (B)*, Vol. 239, No. 2, 2003, pp. 480-489. [doi:10.1002/pssb.200301832](https://doi.org/10.1002/pssb.200301832)
- [15] P. S. Sahoo, A. Panigrahi, S. K. Patri and R. N. P. Choudhary, "Structural, Dielectric, Electrical and Piezoelectric Properties of Ba<sub>4</sub>SrRTi<sub>3</sub>V<sub>7</sub>O<sub>30</sub> (R = Sm, Dy) Ceramics," *Central European Journal of Physics*, Vol. 6, No. 4, 2008, pp. 843-848. [doi:10.2478/s11534-008-0112-3](https://doi.org/10.2478/s11534-008-0112-3)
- [16] K. Kathayat, A. Panigrahi, A. Pandey and S. Kar, "Effect of Holmium Doping in Ba<sub>5</sub>RTi<sub>3</sub>V<sub>7</sub>O<sub>30</sub> (R = Rare Earth Element) Compound," *Integrated Ferroelectrics*, Vol. 118, No. 1, 2010, pp. 8-15. [doi:10.1080/10584587.2010.489461](https://doi.org/10.1080/10584587.2010.489461)
- [17] E. Wu, "POWD, an Interactive Powder Diffraction Data Interpretation and Indexing Program, Version 2.5," School of Physical sciences, Finders University of South Australia, Bedford Park, Australia.
- [18] H. P. Klug and L. E. Alexander, "X-Ray Diffraction Procedures," 2nd Edition, John Wiley & Sons Inc., New York, 1974.
- [19] J. R. Macdonald, "Impedance Spectroscopy-Emphasizing Solid Materials and Synthesis," In: J. R. Macdonald, Ed., *Theory*, John Wiley and Sons Inc., New York, 1987, pp. 13, 77.
- [20] P. S. Sahoo, A. Panigrahi, S. K. Patri and R. N. P. Choudhary, "Structural and Impedance Properties of Ba<sub>5</sub>DyTi<sub>3</sub>-V<sub>7</sub>O<sub>30</sub>," *Journal of Material Science: Material in Electronics*, Vol. 20, No. 6, 2009, pp. 565-570. [doi:10.1007/s10854-008-9766-2](https://doi.org/10.1007/s10854-008-9766-2)
- [21] E. V. Ramana, S. V. Suryanarayana and T. B. Sankaram, "ac Impedance Studies on Ferromagnetic SrBi<sub>5-x</sub>-La<sub>x</sub>Ti<sub>4</sub>FeO<sub>18</sub> Ceramics," *Material Research Bulletin*, Vol. 41, No. 6, 2006, pp. 1077-1088. [doi:10.1016/j.materresbull.2005.11.013](https://doi.org/10.1016/j.materresbull.2005.11.013)

- [22] Z. G. Yi, Q. F. Fang, X. P. Wang and G. G. Zhang, "Dielectric Relaxation Studies on the Submicron Crystalline La<sub>2</sub>Mo<sub>2</sub>O<sub>9</sub> Oxide-Ion Conductors," *Solid State Ionics*, Vol. 160, No. 1-2, 2003, pp. 117-124. [doi:10.1016/S0167-2738\(03\)00143-7](https://doi.org/10.1016/S0167-2738(03)00143-7)
- [23] F. Borsa, D. R. Torgeson, S. W. Martin and H. K. Patel, "Relaxation and Fluctuations in Glassy Fast-Ion Conductors: Wide-Frequency-Range NMR and Conductivity Measurements," *Physical Review B*, Vol. 46, No. 2, 1992, pp. 795-800. [doi:10.1103/PhysRevB.46.795](https://doi.org/10.1103/PhysRevB.46.795)
- [24] S. Saha and T. P. Sinha, "Low-Temperature Scaling Behavior of BaFe<sub>0.5</sub>Nb<sub>0.5</sub>O<sub>3</sub>," *Physical Review B*, Vol. 65, No. 13, 2002, Article ID: 134103. [doi:10.1103/PhysRevB.65.134103](https://doi.org/10.1103/PhysRevB.65.134103)
- [25] S. Sen, P. Pramanik and R. N. P. Choudhary, "Impedance Spectroscopy Study of the Nanocrystalline Ferroelectric (PbMg)(ZrTi)O<sub>3</sub> System," *Applied Physics A: Materials Science & Processing*, Vol. 82, No. 3, 2006, pp. 549-557. [doi:10.1007/s00339-005-3330-1](https://doi.org/10.1007/s00339-005-3330-1)